Theoretical efficiency limits for thermoradiative energy conversion

Rune Strandberg

Citation: Journal of Applied Physics **117**, 055105 (2015); doi: 10.1063/1.4907392
View online: http://dx.doi.org/10.1063/1.4907392
View Table of Contents: http://scitation.aip.org/content/aip/journal/jap/117/5?ver=pdfcov
Published by the AIP Publishing

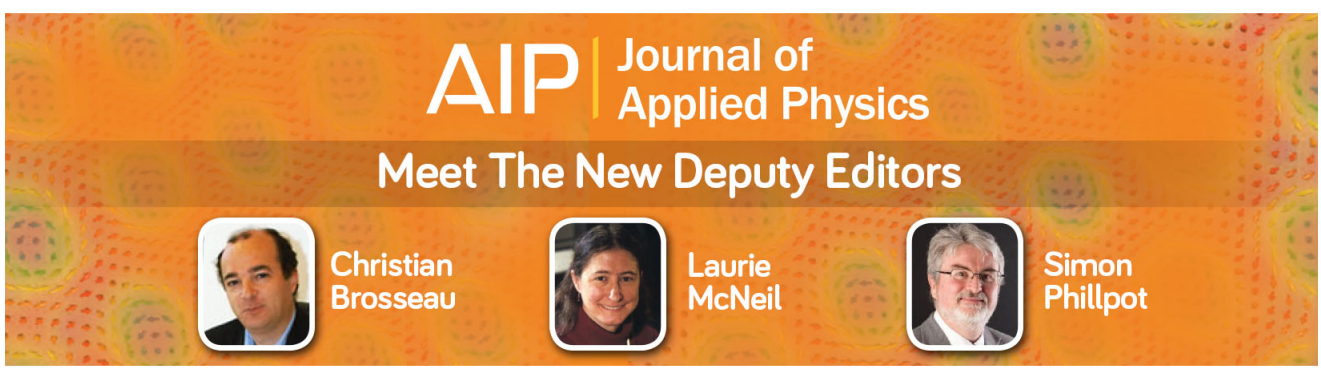

Theoretical efficiency limits for thermoradiative energy conversion

Rune Strandberg[a)]
Department of Engineering Sciences, University of Agder, Jon Lilletuns vei 9, 4879 Grimstad, Norway

(Received 31 October 2014; accepted 22 January 2015; published online 4 February 2015)

A new method to produce electricity from heat called thermoradiative energy conversion is analyzed. The method is based on sustaining a difference in the chemical potential for electron populations above and below an energy gap and let this difference drive a current through an electric circuit. The difference in chemical potential originates from an imbalance in the excitation and de-excitation of electrons across the energy gap. The method has similarities to thermophotovoltaics and conventional photovoltaics. While photovoltaic cells absorb thermal radiation from a body with higher temperature than the cell itself, thermoradiative cells are hot during operation and emit a net outflow of photons to colder surroundings. A thermoradiative cell with an energy gap of 0.25 eV at a temperature of 500 K in surroundings at 300 K is found to have a theoretical efficiency limit of 33.2%. For a high-temperature thermoradiative cell with an energy gap of 0.4 eV, a theoretical efficiency close to 50% is found while the cell produces 1000 W/m^2 has a temperature of 1000 K and is placed in surroundings with a temperature of 300 K. Some aspects related to the practical implementation of the concept are discussed and some challenges are addressed. It is, for example, obvious that there is an upper boundary for the temperature under which solid state devices can work properly over time. No conclusions are drawn with regard to such practical boundaries, because the work is aimed at establishing upper limits for ideal thermoradiative devices. © *2015 AIP Publishing LLC*. [http://dx.doi.org/10.1063/1.4907392]

I. INTRODUCTION

Several technologies have the ability to produce electricity from heat. Of these, thermophotovoltaics and thermophotonic energy conversion are closely related. A thermophotovoltaic cell absorbs thermal radiation from a hotter body and converts a fraction of this into electricity in the same manner as a conventional photovoltaic solar cell. The scientific development of thermophotovoltaics is a bit uncertain, but a historical review can be found in Ref. 1 and a good description of the fundamental physics is found in Ref. 2.

A thermophotonic system consists of a light emitting diode (LED) paired with a photovoltaic cell.[3] Ideal LEDs emits photons with energy close to the band gap energy, even when the energy transferred to each electron by the applied potential is smaller than this band gap energy.[4] To keep an ideal LED in steady state during operation, heat must be supplied. Photons emitted by an LED have spectrum that allows a photovoltaic cell to convert the emitted energy to electricity at high efficiency. In thermophotonic systems, heat plus some electricity is converted into more electricity when an LED emits light onto a photovoltaic cell which produces electricity to be delivered to an electric circuit.

Thermoradiative cells, the concept to be analyzed in this paper, are also based on the physical principles that pave the ground for photovoltaics. A fundamental difference exists, because thermoradiative cells are supposed to be heated to temperatures higher than the ambient temperature during operation. The concept involves converting part of the heat that is supplied to keep the cell at a constant temperature to electricity. A sketch of this is shown in Figure 1. The thermoradiative cell is thus a type of emissive energy harvester as described and discussed in a recent paper by Byrnes *et al.*[5]

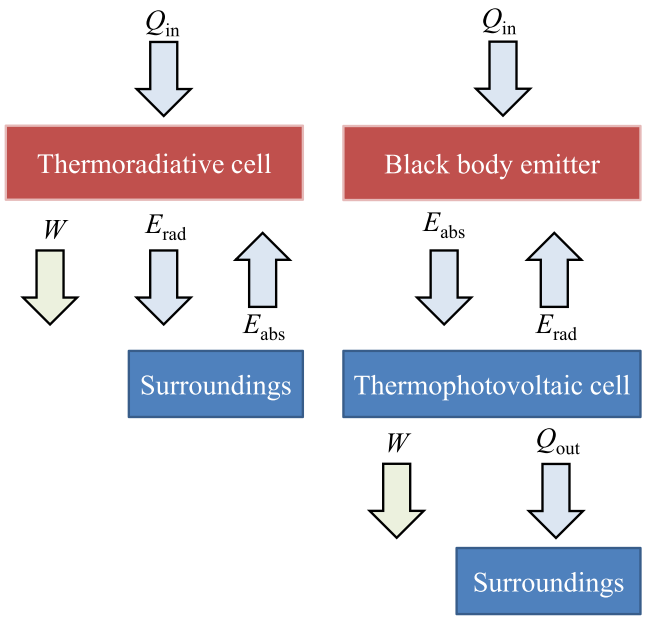

FIG. 1. In an ideal thermoradiative cell, heat Q_{in} and radiative energy E_{abs} is supplied, while work W is delivered and radiative energy E_{rad} is emitted. A thermophotovoltaic cell receives radiative energy from a heated body while producing work and emitting radiative energy. In general, heat must be removed from a thermophotovoltaic cell to prevent its temperature from rising (Q_{out}).

[a)]rune.strandberg@uia.no

As will be explained later, thermoradiative cells deliver power when operated with a negative bias. Green has briefly discussed some relevant issues regarding negatively biased devices in Ref. 2 (p. 121) and concluded that the optical properties of such devices will be dominated by free-carrier transitions instead of band-to-band transitions. To contradict this statement, the present work includes an Appendix where InAs is used as an example to show that free-carrier emission/absorption of photons does not necessarily dominate negatively biased devices.

The scope of this article is to describe the working principle of thermoradiative energy conversion and to calculate theoretical efficiency limits for ideal thermoradiative devices. Issues related to free-carrier emission and other intra-band processes, some aspects regarding implementation of the concept as well as non-ideal losses are also briefly discussed.

II. WORKING PRINCIPLE

When an unbiased semiconductor diode is in thermal equilibrium with its surroundings, the numbers of photons emitted and absorbed by it are in balance. If the temperature of the surroundings is reduced, more photons will be emitted than absorbed by the diode. When photon emission and absorption is restricted to transitions across the band gap, the numbers of electrons and holes are then reduced. This corresponds to a shift in the quasi-Fermi levels of the two types of carriers. Since the starting point was thermal equilibrium, the quasi-Fermi level for the holes must now be higher than that of the electrons. The quasi-Fermi level split will increase until a balance in the emitted and absorbed photon fluxes is re-established. The positioning of the quasi-Fermi levels then corresponds to a negative open circuit voltage.

If the diode is short circuited, a recombination of an electron-hole pair that is not balanced by the generation of another electron-hole pair results in transport of an electron through the circuit. The electron must be extracted from the valence band and inserted to the conduction band. This corresponds to an electric current moving in the negative direction when directions are defined as by convention in photovoltaic literature.

Electrons that have entered the conduction band from an external circuit have to achieve two things before they can leave the cell at the opposite electrode: (1) De-excite across the band gap. (2) Increase their energy by intra-band thermal excitation. In Figure 2, a possible route for an electron going through the cell is sketched. After the de-excitation to the valence band has taken place, there are two ways for the electron to get back to the conduction band. It can either be re-excited across the band gap or go through the external circuit. The number of electrons taking either of these two routes will be calculated later. The electron population in each band is distributed according to Fermi–Dirac statistics. Whenever an electron is extracted to the external circuit, the remaining valence band electrons are redistributed to maintain the Fermi–Dirac distribution. The redistribution assures a continuous flow of electrons being thermally excited to the valence band edge on the p-side of the diode.

Implementations of the thermoradiative concept which are not based on semiconductors might exist. In the following, the term *energy gap* is therefore used when treating the concept of thermoradiative energy conversion in general, and the term *band gap* is used when discussing semiconductor based implementations.

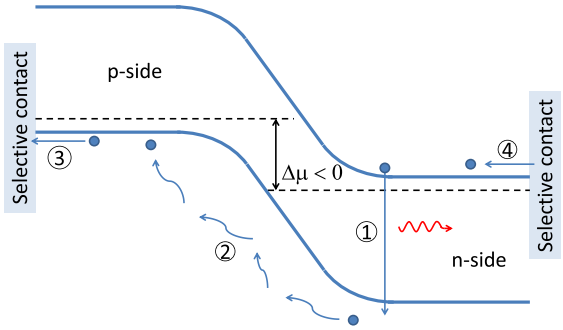

FIG. 2. Sketch showing a possible route for an electron going through the cell. (1) An electron-hole pair recombines radiatively over the band gap. (2) The electron increases its energy by thermal excitations due to redistribution of the electron population when electrons leave the cell. (3) Electron extraction to an external circuit via a metallic contact, leaving a hole behind. (4) The electron completes the loop when it is re-inserted to the conduction band of the cell.

In most of this paper, ideal thermoradiative cells are considered. This implies that the cells are assumed to possess the following properties: (I) The main part of the cell consists of an active material that has an energy gap over which electrons can only be excited by photons. De-excitations over the energy gap are only allowed if the excess energy is emitted as a photon. (II) The cell is a perfect absorber and emitter of photons with energy larger than the energy gap. The absorptivity for photons with energy lower than the energy gap is zero. (III) Electrons can be inserted to electron states above the energy gap by an ideal contact. The ideal contact ensures lossless transport of electrons between these states and an external electric circuit. Similarly, another ideal contact can extract electrons from electron states below the energy gap. (IV) Electrons can move inside the thermoradiative cell without loss of energy. (V) The back side of the device should be a perfect reflector.

Note that the properties above are similar to those assumed for an ideal photovoltaic cell.[6] An example of a structure that fulfills the above requirements is thus an ideal semiconductor diode. Using pn-junction diodes as emissive energy harvesters has already been proposed by Byrnes *et al.*,[5] but efficiency limits have not been established previously.

For photovoltaic cells, the purpose of the back side reflector is to assure recycling of photons emitted by the cell in the backward direction. For a thermoradiative cell, the reflector serves as a layer of optical insulation, preventing emission of photons from the heat source to the cell, where it would cause performance degrading excitation of electrons across the energy gap. The reflector also prevents emission of sub-energy gap photons.

III. MATHEMATICAL MODEL

Assumption II allows us to find the net rate of electrons crossing the energy gap. In line with the detailed balance formalism, first applied by Shockley and Queisser when

calculating the limiting efficiency of photovoltaic cells,[6] the number of electrons delivered by the cell to an external circuit equals the net absorption of photons. This gives a current density

$$I = q[\dot{N}(T_a, 0) - \dot{N}(T_c, \Delta\mu_c)], \tag{1}$$

where T_c is the cell temperature, T_a the ambient temperature, and q is the elementary charge. $\Delta\mu_c$ is the split between the quasi-Fermi levels for electrons and holes, which are assumed to be constant throughout the entire cell, as a consequence of assumption IV. $\dot{N}(T_c, \Delta\mu_c)$ is the flux of photons emitted by the cell to the surroundings, and $\dot{N}(T_a, 0)$ is the flux of photons from the surroundings that are absorbed by the cell. The photon flux emitted from a point on a surface is given by[7]

$$\dot{N}(T, \Delta\mu) = \frac{2\pi}{h^3c^2}\int_{E_g}^{\infty} \frac{\varepsilon^2}{\exp[(\varepsilon - \Delta\mu_c)/kT] - 1}\, d\varepsilon, \tag{2}$$

where k is Boltzmann's constant, T is the temperature of the surface, and $\Delta\mu_c$ is the chemical potential driving the emission. The integral is taken over the photon energy ε. All the radiation emitted from a point on a flat or convex surface or will be emitted to the surroundings. Multiplying Eq. (2) by the area of surface that is not self-illuminating gives the total number of photons emitted by the surface to the surroundings per unit time. Equation (2) also describes the flux of photons impinging a point on a flat or convex surface placed in surroundings emitting like a black body with the temperature T.

In semiconductor physics, it is well known that the voltage V between the cell's two contacts is given by $V = \Delta\mu_c/q$, so the power density of the energy delivered to the external circuit equals

$$P = IV = \Delta\mu_c[\dot{N}(T_a, 0) - \dot{N}(T_c, \Delta\mu_c)]. \tag{3}$$

Photovoltaic and thermophotovoltaic cells operate in the first quadrant of the current-voltage (IV) diagram shown in Figure 3. Since the current and voltage are both positive in this quadrant, so is the power production. In Sec. II, it was explained that thermoradiative cells operate with a negative current as well as a negative voltage. The thermoradiative region of the IV-diagram is therefore found in the third quadrant, which is also a power producing quadrant. The IV-curve of a thermoradiative cell, as described by Eq. (1), is plotted in Figure 3 along with an IV-curve of a thermophotovoltaic cell with similar characteristics.

In the following, the efficiency η of a thermoradiative cell is defined as the ratio of the electric output power to the supplied heat, that is

$$\eta = \frac{P}{\dot{Q}_{in}} = \frac{P}{P + \dot{E}_{rad} - \dot{E}_{abs}}, \tag{4}$$

where $\dot{E}_{rad} = \dot{E}_{ph}(T_c, \Delta\mu_c)$ is the radiative energy flux emitted by the cell, and $\dot{E}_{abs} = \dot{E}_{ph}(T_a, 0)$ is the radiative energy flux absorbed by the cell. $\dot{Q}_{in}$ is the heat flux required to maintain the cell at a constant temperature. $\dot{E}_{ph}(T, \Delta\mu)$ is given by

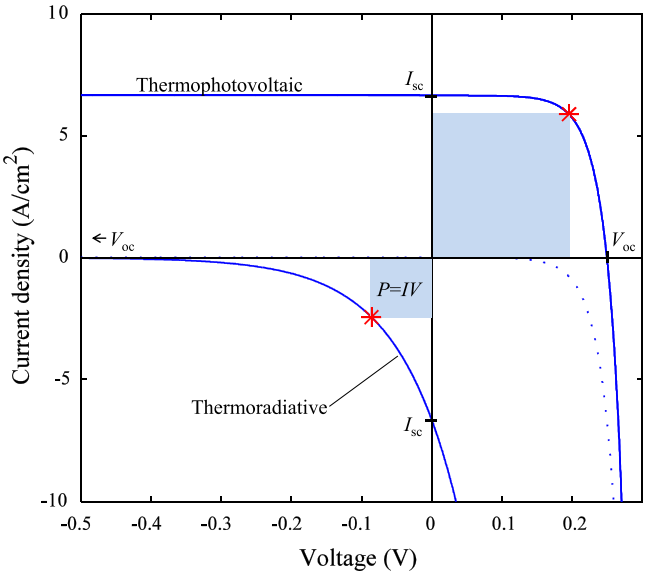

FIG. 3. IV-curves of a thermoradiative cell and a thermophotovoltaic cell with an energy gap of 0.3 eV. The thermoradiative cell has a temperature of 1000 K while the ambient temperature is 300 K. The thermophotovoltaic cell receives radiation from a 1000 K black body that is illuminating the cell over a hemisphere. The maximum power points are shown by stars. The dotted line shows the IV-curve, for both devices, when in thermal equilibrium with their surroundings at 300 K.

$$\dot{E}_{ph}(T, \Delta\mu) = \frac{2\pi}{h^3c^2}\int_{E_g}^{\infty} \frac{\varepsilon^3}{\exp[(\varepsilon - \Delta\mu)/kT] - 1}\, d\varepsilon. \tag{5}$$

The validity of Eq. (5) is seen from Eq. (2) and noting that each photon carries an energy ε. Readers familiar with photovoltaic theory will notice that all of the above equations, except the definition of the efficiency, are similar to the relevant equations for photovoltaic and thermophotovoltaic devices. Any photon with energy lower than the energy gap emitted by the cell will add to the denominator in 4 and reduce the cell efficiency, while the output power remains unchanged. Photons with energy larger than the energy gap that are emitted in intra-band processes suppress the number of photons emitted by inter-band processes since the total emissivity for any photon energy cannot be larger than one. Such intra-band emissions will thus reduce both efficiency and power.

In photovoltaic devices the maximum power point (MPP) coincides with the highest efficiency, because the efficiency is calculated as the ratio of the work to the incoming radiative energy, the latter being a fixed quantity. For thermoradiative devices, the heat flux required to maintain a stable temperature varies with the energy flux radiated by the cell, which depends on the cell voltage. The highest efficiency is therefore found at a maximum efficiency point (MEP), which, in general, is different from the MPP.

IV. RESULTS

Figure 4 shows how the calculated efficiency varies with the cell voltage for cells with a temperature of 1000 K placed

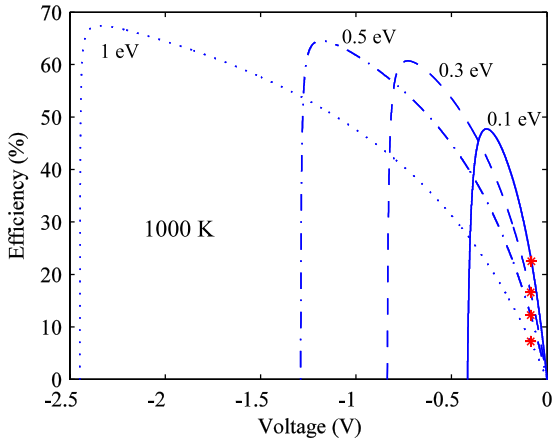

FIG. 4. The efficiency for cells with four different energy gaps plotted as a function of the cell voltage. The cell temperatures are 1000 K and the ambient temperature is 300 K. The stars indicate the maximum power points.

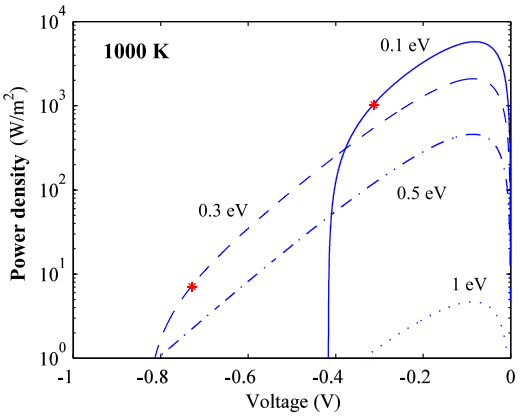

FIG. 6. The output power density for four cells with different energy gaps plotted as a function of the cell voltage. The cell temperature is 1000 K and the ambient temperature is 300 K. The stars indicate the MEP. For energy gaps of 0.5 eV and 1 eV, the power density at the MEP is too low to be shown in this plot.

in surroundings with a temperature of 300 K. Plots are shown for four different energy gaps, and the maximum power points are indicated by stars. A similar chart with values calculated with a cell temperature of 500 K is shown in Figure 5. Note that the efficiency at the MEP increases with the energy gap of the cell, while the efficiency at the MPP decreases. Note also that there can be a large difference between the efficiency at the MEP and the efficiency at the MPP. In Appendix A it is shown that the maximum efficiency approaches the Carnot efficiency when the energy gap becomes very large.

Plots of the output power density as a function of the cell voltage are shown in Figures 6 and 7. It becomes evident that the maximum power density decreases rapidly with the size of the energy gap, and that the power density at the MPP is several times larger than the power at the MEP.

Determination of the optimal point of operation is a trade-off between power and efficiency. From the data plotted in Figures 4 and 6, where the cell temperature is 1000 K, it is found that an ideal cell with an energy gap of 0.3 eV has an efficiency of 35.4% when it delivers 1000 W/m^2. A cell with an energy gap of 0.5 eV can produce 300 W/m^2 at 30.8% efficiency. This power density and efficiency is, by coincidence, close to the power density and efficiency of an ideal single band gap photovoltaic cell illuminated by unconcentrated sunlight. With a cell temperature of 500 K, the power is drastically reduced and the energy gap has to be below 0.17 eV to allow a maximum power density above 100 W/m^2. Typical peak efficiencies ranges from 25% to 35% for energy gaps between 0.1 and 0.3 eV.

Figure 8 shows the *efficiency* at the MEP and MPP as a function of the energy gap for cell temperatures of 500 K, 750 K, and 1000 K. For the same cases, Figure 9 shows the *power density* at the MEP and MPP. The plots thus display the ranges of power density and efficiency that are achievable for voltages between the MEP and MPP. It is seen from the figures that small energy gaps give high power and low peak efficiency, while larger energy gaps give higher peak efficiency, but less power. Considering semiconductors with a small band gap, free-carrier emission will compete with radiative inter-band transitions at energies above the energy gap and reduce the output power of the cell. In addition, non-radiative inter-band processes like multi-phonon recombination will reduce the open circuit voltage of the cell. The

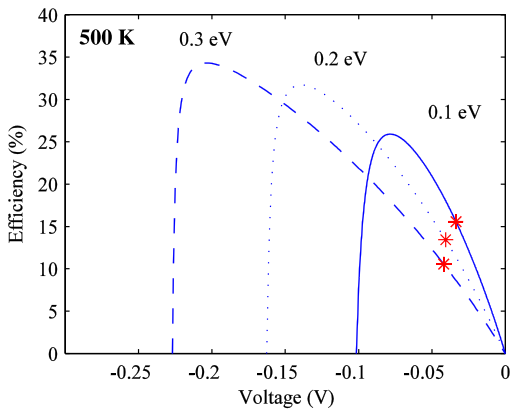

FIG. 5. The efficiency for cells with three different energy gaps plotted as a function of the cell voltage. The cell temperatures are 500 K and the ambient temperature is 300 K. The stars indicate the maximum power points.

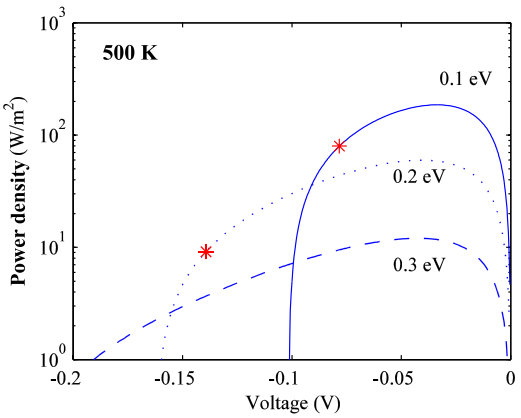

FIG. 7. The output power density for three cells with different energy gaps plotted as a function of the cell voltage. The cell temperature is 500 K and the ambient temperature is 300 K. The stars indicate the MEP. For an energy gap of 0.3 eV, the power density at the MEP is too low to be shown in this plot.

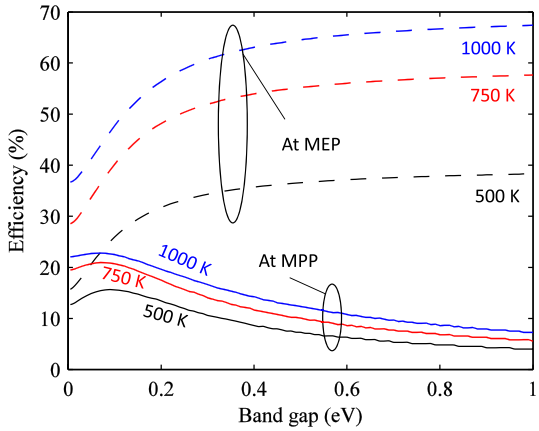

FIG. 8. The efficiency at the MPP and MEP plotted as a function of the energy gap for cell temperatures of 500 K, 750 K, and 1000 K. The ambient temperature is set to 300 K.

results in Figures 8 and 9 are thus of little practical interest for semiconductor based devices with very small band gaps. At some point, however, the band gap is sufficiently large for radiative recombination to be the dominating inter-band mechanism. Sub-band gap free-carrier emission and other sub-band gap processes will not reduce the cell power, but will add to the denominator in Eq. (4) and reduce the conversion efficiency of the cell.

The power densities in Figure 9 can be compared to the power density achieved by photovoltaics. A typical commercial solar cell with 17% efficiency has a yearly average power density of 29 W/m^2 when placed at a location where the annual yield is 1500 kWh/kW_p which is typical for Southern Europe and the Southeastern United States.

Any electron that is excited across the energy gap of a thermoradiative cell in a non-radiative process will reduce the current delivered by the cell. This could be Auger excitations, excitations via impurity states in the band gap or multi-phonon excitations. With a negative bias, a thermoradiative cell might have a net excitation across the energy gap due to non-radiative processes. The sum of this net rate and the radiative excitation rate can be expressed as a multiple of the radiative excitation rate. The sensitivity of a thermoradiative cell to non-radiative processes can then be investigated by a simple modification of Eq. (1). Multiplying $\dot{N}(T_a, 0)$ by 1, 10, or 100 implies looking at cases where radiative excitation contributes to 100%, 10%, and 1%, respectively, of the total excitation rate. Note that the net rate of the different excitation processes can have varying voltage dependencies. The percentage of radiative excitation can therefore vary along the IV-curve. Fixed values, which are used here, can still be used since we are only interested in the efficiency at one particular voltage—the one giving the highest power density. Figure 10 shows how the power density at the MPP changes when the amount of non-radiative excitation increases. Table I lists the highest achievable power density and efficiency at the MPP for the same and some additional cases. One can see from the figure that the impact of non-radiative excitation decreases with the band gap of the cell. For larger band gaps, the radiative excitation rate is small compared to the rate of radiative de-excitation and multiplying it by 10 or 100 does not alter the IV-curve substantially. It is also seen from Figure 10 that the cell performance becomes less sensitive to non-radiative excitation with increasing temperature. Higher temperatures give more radiative de-excitation, which means that more non-radiative excitation is needed to change the IV-curve significantly.

For cells with a temperature of 750 K, it is seen from the values in Table I that power densities higher than that of typical photovoltaic solar cells can be achieved even when the radiative excitation rate is only 0.01% of the total excitation rate. For cells with a temperature of 500 K, close to 10% of the excitation must be radiative to achieve power densities above the average annual power density for typical photovoltaic solar cells.

V. DISCUSSION OF PRACTICAL IMPLEMENTATION

Any dark, cold surface can constitute the cold side of a thermoradiative system. If this surface is sufficiently large compared to the size of the cell, there is no need for active cooling of the cold side. This is an advantage of thermoradiative systems over systems where active cooling of the cold

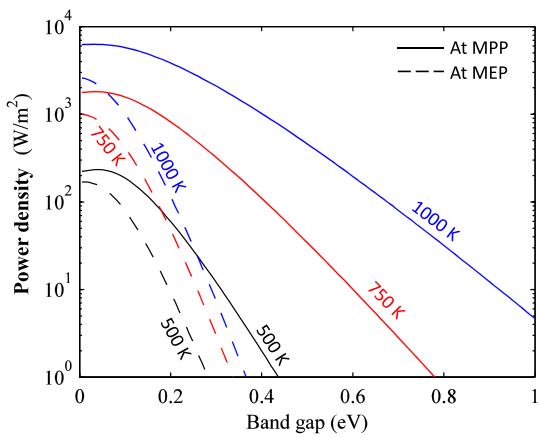

FIG. 9. The power density at the MPP and MEP plotted as a function of the energy gap for cell temperatures of 500 K, 750 K, and 1000 K. The ambient temperature is set to 300 K.

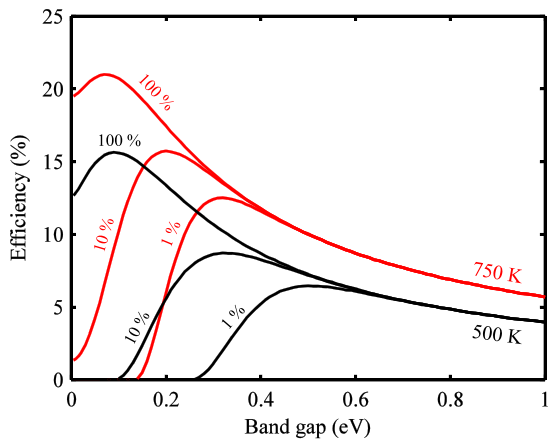

FIG. 10. The cell efficiency plotted as a function of the energy gap for cells where radiative excitation makes up 100%, 10%, and 1% of the total excitation rate. Plots are shown for cell temperatures of 500 K and 750 K.

TABLE I. Maximum power density and maximum efficiency at the MPP for cells with different percentages of radiative excitation. The band gaps giving these maximum values are also listed.

Temperature(K)	Percentage radiative excitation (%)	Maximum power density(W/m^2)	E_g at maximumpower density(eV)	Maximum efficiency (%)	E_g at maximum efficiency (eV)
500	100	234	0.04	15.6	0.09
500	10	34.9	0.18	8.7	0.32
500	1	2.7	0.33	6.5	0.50
750	100	1806	0.04	21.0	0.07
750	10	1022	0.13	15.7	0.20
750	1	431	0.23	12.5	0.32
750	0.1	156	0.33	10.4	0.43
750	0.01	50.8	0.43	8.9	0.53

side is required. A comparative disadvantage of thermoradiative cells with respect to thermophotovoltaics, is that the electrical connections are found at the hot side of the system. And any heat lost by conductive or convective cooling of the cell will add to the denominator in Eq. (4) and reduce the conversion efficiency.

When dealing with common semiconductors at room temperature, the band gap is much larger than the typical phonon energy. Therefore, phonons cannot excite electrons across the band gap, unless in multi-particle processes which will only happen at very low rates. With higher temperatures and lower band gaps, the probability and rates of inter-band excitations induced by phonons will increase. In a thermoradiative cell, such excitations lead to reductions in the current which will reduce the cell efficiency. Since the typical energy of an optical phonon in a semiconductor is around 50 meV or less, such excitations will still be multi-particle processes even for rather small band gaps.

Free-electron emission of sub-band gap photons also represents a non-ideal loss of energy which will lower the conversion efficiency of thermoradiative cells. In semiconductors, the impact of free-electron emission increases with temperature. The absorption coefficient for sub-bandgap photons can still be significantly lower than the absorption coefficient related to inter-band transitions even at several hundred Kelvin.[8] The impact of free-electron emission can therefore, at least in principle, be limited by choosing an appropriate thickness of the active layer to assure an almost transparent cell in the sub-band gap range and good opacity for photons with energy larger than the band gap. To assure minimal impact of free-carrier emission, the active region of semiconductor based thermoradiative cells should be made of intrinsic material which has the minimum possible concentration of charge carriers. A p-i-n device with small p- and n-regions around point contacts that cover as little as possible of the back side of the cell could be an appropriate design. The negative bias experienced by thermoradiative cells during operation will reduce the number of free-carriers and thereby also the free-carrier emission.

Using data from Refs. 8–10 on the sub-band gap absorption of InAs, it is possible to model how sub-band gap emission impacts an InAs-based thermoradiative cell. A rough, and conservative rather than accurate, model of this kind is presented in Appendix B. The model shows that emission of sub-band gap photons can have a significant impact on the efficiency, but this impact is not necessarily detrimental.

The ideal thermoradiative cell should have a perfectly reflective back side. Due to free-carrier emission, metallic reflectors are not well suited. One possibility is to use infrared dielectric omnidirectional reflectors.[11]

When operating solid state devices at elevated temperatures, changes in atomic structure, enhanced diffusion of impurities and dopants, and possibly other processes, are challenges to be addressed. An analysis of the impact of such issues, as well as evaluating the possibility of overcoming them, is beyond the scope of the present work. Whether useful thermoradiative cells can be made or not is a question that cannot be answered at present and further work is required.

VI. CONCLUSION

This paper presents the fundamental principles of thermoradiative energy conversion. It is shown how theoretical efficiency limits can be calculated using detailed balance calculations. The results of such calculations show that ideal thermoradiative cells can produce electricity with power densities comparable to that of photovoltaics, when the temperature of the thermoradiative cell is 500 K. With increasing cell temperature, both power density and conversion efficiency increase.

Several issues that will reduce the efficiency of non-ideal thermoradiative devices have been pointed out. Most of the performance degrading processes, including radiative intra-band transitions and convective and conductive heat losses, will generally increase in intensity with increasing cell temperature, as will issues related to material stability. On the other hand, cells operated at higher temperatures are shown to be less sensitive to non-radiative excitation of electrons from the valence band to the conduction band. The paper does not make any conclusions regarding the possibility of producing real thermoradiative cells with efficiencies sufficiently high to be useful.

ACKNOWLEDGMENTS

The author would like to thank Dr. Thomas R. Harris at the Airforce Institute of Technology for providing valuable details on the measurements in Ref. 8.

APPENDIX A: PROOF SHOWING THAT THE EFFICIENCY CAN APPROACH THE CARNOT LIMIT FOR LARGE BAND GAPS

If $\Delta\mu_c < 0$ and the energy gap is much larger than kT, then $\varepsilon - \Delta\mu_c \gg kT$ for $\varepsilon > E_g$, which gives $\exp[(\varepsilon - \Delta\mu_c)/kT] - 1 \approx \exp[(\varepsilon - \Delta\mu_c)/kT]$. Using this approximation in Eqs. (2) and (5) gives integrals with analytical solutions. The resulting expressions for the photon fluxes and radiative energy flux becomes

$$\dot{N}(T,\Delta\mu_c) \approx \frac{2\pi kT}{h^3c^2}\left[E_g^2 + 2kTE_g + 2(kT)^2\right]e^{\frac{\Delta\mu_c - E_g}{kT}} \approx \frac{2\pi kT}{h^3c^2}E_g^2 e^{\frac{\Delta\mu_c - E_g}{kT}} \text{ and} \tag{A1}$$

$$\dot{E}_{ph}(T,\Delta\mu_c) \approx \frac{2\pi kT}{h^3c^2}\left[E_g^3 + 3kTE_g^2 + 6(kT)^2E_g + 6(kT)^3\right] \times e^{\frac{\Delta\mu_c - E_g}{kT}} \approx \frac{2\pi kT}{h^3c^2}E_g^3 e^{\frac{\Delta\mu_c - E_g}{kT}}. \tag{A2}$$

Since E_g is already assumed to be much larger than kT, the first term in the brackets in Eqs. (A1) and (A2) is much larger than the other terms, which can be omitted. Inserting the resulting approximations into the relevant expressions for the terms in Eq. (4) gives

$$\eta \approx \frac{\Delta\mu_c}{\Delta\mu_c - E_g}, \tag{A3}$$

after some algebraic manipulation.

Using the approximations in Eqs. (A1) and (A2), still omitting small terms, one gets

$$I \approx \frac{2\pi kE_g^2}{h^3c^2}\left(T_c e^{-\left(E_g - \Delta\mu_{c,Voc}\right)/kT_c} - T_a e^{-E_g/kT_a}\right) = 0, \tag{A4}$$

at the open circuit voltage. Solving Eq. (A4) for $\Delta\mu_{c,Voc}$, the quasi-Fermi level split at V_{oc}, gives

$$\Delta\mu_{c,Voc} \approx E_g\left(1 - \frac{T_c}{T_a}\right). \tag{A5}$$

Inserting this into Eq. (A3), it is found that as the voltage approaches the open circuit voltage, the efficiency approaches

$$\eta = 1 - \frac{T_a}{T_c}, \tag{A6}$$

which is the Carnot efficiency. Note that the output power goes towards zero when the voltage approaches the open circuit voltage.

APPENDIX B: A SIMPLIFIED MODEL FOR FREE-CARRIER EMISSION IN INAS

The impact of sub-band gap emission is here studied by a simplified model based on the absorption coefficient of InAs at 500 K. The band gap of InAs at 500 K is 0.26 eV.[8] For these calculations, the sub-band gap absorption coefficient of InAs is modeled differently in two intervals. The upper interval goes from 70 meV to 0.26 eV. For this interval, experimental values from the work of Harris[8] are used directly. The thickness of the sample used in the cited work was 850 μm,[12] which makes extraction of the absorption coefficient straight forward. Surface absorption, impurity absorption, and reflection might lead to an overestimation of the absorption coefficient using these measurements.[12] The extracted values can therefore be considered conservative. Between 70 meV and 0.26 eV, the absorption coefficient calculated these measurements has values between 35 cm^{-1} and 75 cm^{-1} at 500 K.

Below 70 meV, the absorption coefficient at 500 K is modeled using an empirical power law for free-carrier emission. The sub-band gap absorption coefficient for lightly doped InAs-samples found in Refs. 10 and 9 is proportional to $\lambda^{2.6}$, where λ is the wavelength of the radiation, at 300 K. A power law relationship between absorption coefficient and wavelength is expected from the theory of free-carrier absorption.[13] In this simplified model for InAs, the $\lambda^{2.6}$ dependency has been used from 70 meV and below. This is likely to give an overestimation of the absorption coefficients because the absorption coefficient found from Harris' work does not increase that rapidly with the wavelength when the photon energy is around 70 meV.

The room temperature absorption coefficient of InAs quickly reaches 3000 cm^{-1} as soon as the photon energy gets above the band gap of the material. A constant value of the absorption coefficient of 3000 cm^{-1} is therefore used for inter-band transitions. A cell thickness of 5 μm is further assumed. This assures an absorptivity of 0.95 for photons with energy above the band gap impinging the cell normal to its surface. In this simplified model, the integrands in Eqs. (2) and (5) are multiplied by the energy dependent absorptivity perpendicular to the cell surface, equaling $1 - \exp[-2\alpha(\varepsilon)W]$, where $\alpha(\varepsilon)$ is the energy dependent absorption coefficient and W is the cell thickness. The lower integration limit of Eq. (5) is changed to 0. This is a simplification, because the

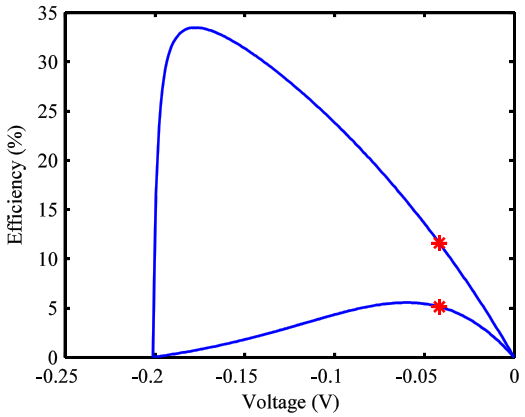

FIG. 11. The efficiency of an ideal thermoradiative cell with a band gap of 0.26 (solid line) and a cell with sub-band gap emission based on the properties of InAs (dashed line). The cell temperature is set to 500 K. The maximum power points are marked by stars.

absorptivity generally depends on the direction of the radiation and the geometry of the cell. Besides this, the modeling is carried out similarly to the calculations presented earlier in this article.

Figure 11 shows a plot of the efficiency calculated with and without sub-band gap emission with the cell temperature set to 500 K. From the figure, it becomes clear that the efficiency is approximately halved at the maximum power point. The 500 K absorption spectrum from Ref. 8 shows that the absorption coefficients from free-carrier emission and other intra-band processes are small at photon energies close to the band gap. Therefore, the power delivered by the cell is not noticeably impacted by such processes, although the efficiency is. Note that the impact of sub-band gap emission can be reduced if spectrally selective reflectors are used to reflect this radiation back to the cell.

It should be emphasized that a proper evaluation of InAs as a thermoradiative material requires a more detailed analysis.

[1]R. E. Nelson, Semicond. Sci. Technol. **18**, S141 (2003).
[2]M. A. Green, *Third Generation Photovoltaics* (Springer-Verlag, Berlin, Heidelberg, 2003).
[3]N. Harder, D. Neuhaus, P. Würfel, A. Eberle, and M. Green, in *Proceedings of the 17th European Photovoltaic Solar Energy Conference and Exhibition*, Munich, Germany (2001), pp. 102–106.
[4]G. Dousmanis, C. Mueller, H. Nelson, and K. Petzinger, Phys. Rev. **133**, A316 (1964).
[5]S. J. Byrnes, R. Blanchard, and F. Capasso, Proc. Natl. Acad. Sci. U. S. A. **111**, 3927 (2014).
[6]W. Shockley and H. J. Queisser, J. Appl. Phys. **32**, 510 (1961).
[7]A. Vos and H. Pauwels, Appl. Phys. **25**, 119 (1981).
[8]T. R. Harris, "Optical properties of Si, Ge, GaAs, GaSb, InAs, and InP at elevated temperatures," Master thesis (Air Force Institute of Technology, 2010).
[9]E. D. Palik, *Handbook of Optical Constants of Solids* (Academic Press Inc., 1985).
[10]R. M. Culpepper and J. R. Dixon, J. Opt. Soc. Am. **58**, 96 (1968).
[11]Y. Fink, J. N. Winn, S. Fan, C. Chen, J. Michel, J. D. Joannopoulos, and E. L. Thomas, Science **282**, 1679 (1998).
[12]T. R. Harris, private communication, Airforce Institute of Technology (2014).
[13]S. Elliott, *The Physics and Chemistry of Solids* (John Wiley and Sons, 2000).